Structural Dynamics, Krätzig et al. (eds), © 1990 Balkema, Rotterdam. ISBN 90 6191 168 0

Soil stiffness and damping

M. D. Bolton & J. M. R. Wilson
Cambridge University, UK

ABSTRACT: Fast and slow cyclic tests on sand have revealed that the stiffness and damping of the soil skeleton are truly hysteretic, and independent of rate of strain. Silicone oil as pore fluid increases damping, but water has a negligible effect even at frequencies higher than those of typical of earthquakes.A body of hysteretic material is found to be very sensitive to the frequency of excitation just below resonance.

1 INTRODUCTION

Dynamic analyses of soil usually assume that it can be treated as a visco-elastic material. Although it is recognized that shear stiffness G must be taken to reduce with increasing strain, most analysts would be content to select an equivalent linear elastic modulus, taking into account the expected magnitudes of initial density, mean effective stress and shear strain.

Energy absorption in soils leads, in current practice, to the definition of an equivalent viscous damping ratio D . This is often determined from the ratio of amplitudes a of successive cycles of the decay of a free oscillation. It may be shown that $D = 1 / (1 + 2\pi / \ln(a_n / a_{n+1}))$ for a perfect visco-elastic element. To be self-consistent, such a value should be proportional to the frequency of oscillations of given amplitude. Some authors have remarked on the absence of such a variation (Iwasaki et al, 1978) leading them to propose that soils can be treated not as viscous, but as hysteretic – absorbing energy solely as a function of cyclic strain. Others treat soils as truly viscous and draw a parallel between dynamic damping and long term creep (Abbiss, 1986).

Two fundamental problems emerge. First, total soil damping should be divided into two components, one (presumably hysteretic) due to the aggregate and one (presumably viscous) due to the pore fluid. Then the constitutive parameters could describe the transition from hysteretic behaviour at low frequencies to partly viscous behaviour at high frequencies. Second, the dynamic behaviour of soil systems should be investigated using a truly hysteretic model for aggregate behaviour. Only then can predictions be made of systems in which changes of stiffness lead to changes of natural frequency, and thereby to changes of response amplitude which in turn lead to further changes of stiffness. Instability might occur if the natural frequency drops to the excitation frequency.

2 SOIL TESTING APPARATUS

Solid cylindrical soil samples were tested in torsion at two strain rates, one fast enough to encompass earthquake effects, for example, and one so slow as to be quasi-static. Two pieces of apparatus were used, the Stokoe rig for resonant column tests and the Wilson rig for slow cyclic tests. Both rigs were constructed in the Engineering Department of Cambridge University, the first to a design kindly supplied by K.H.Stokoe (University of Texas). Soil samples were all 38 mm diameter and 78 mm high, and boundary conditions were identical in each apparatus. If precise parameters had been required for design purposes, then it might have been necessary to use larger, hollow cylindrical samples in which the variation of shear strain with radius would have been negligible. For the purposes of investigating strain-rate effects, the simplicity of solid samples was preferred.

The Stokoe Apparatus is shown in cross-section in Fig. 1; numbers in brackets refer to the numbered components. The sample (5) is enclosed in a rubber membrane placed between a lower platen (3) and a top cap (6), both of which were roughened to provide torsional coupling. A cruciform loading arm (7) carries permanent magnets (8) which can oscillate freely within coils (9). The coil assembly is mounted on an adjustable holding ring (10) supported by an outer sleeve (11). All this is enclosed within a pressure sleeve (12) and end plates (1 and 13), retained by tension bolts (14). Cell pressure is provided by compressed air. Pore pressures may be measured by connecting a line (2) through the base.

This resonant column apparatus was used for two types of test – frequency response tests and free decay tests – both under the control of a micro-computer. For frequency response, a fixed amplitude sinusoidal torque was applied to the sample at a sequence of frequencies increasing from 20 Hz to

110 Hz in 1 Hz increments so that the resonant frequency could be established with reasonable accuracy. An accelerometer fixed to the top platen was used to record the response in the last 100 cycles of a 1000 cycle input at each frequency. The signal was integrated twice to obtain top-cap rotation: numerical integration was checked electronically. Both driving current (calibrated against torque) and acceleration were logged at 32 points per cycle. Free decay tests were then conducted by opening the circuit to the driving coils following 1000 cycles of input at the resonant frequency. Data of the last 5 powered cycles, and the succeeding decay of vibrations, was recorded. Similar frequency response sweeps and free decay trials were carried out at various amplitudes of input current.

The Wilson Apparatus is shown in cross-section in Fig. 2. The soil sample (1) is retained between roughened platens on the top-cap (4) and pedestal (2) which incorporates a torsional load cell (3). The bearings (6) on the top platen assembly permit vertical movement without axial rotation. Torque is applied to the lower platen by the stepper motor (7), relative rotation being measured by an LVDT (8). Experiments were performed under compressed air within a pressure vessel (9). Both load and strain control were effected through a micro-computer. One motor step corresponded to about 10^{-5} nominal shear strain. LVDT and load cell readings were averaged in the interval 1 to 2 seconds after each step, and recorded with 12 bit accuracy.

3 CYCLIC DATA FOR DRY SAND

Samples of Leighton Buzzard (14/25) sand were prepared dry by axial pouring. Only one void ratio out of 22 fell outside the range 0.575 ± 0.025. All the data to be presented therefore refer to quartz sand at a relative density of about 75%.

Fig. 3 compares the "backbone" data of torque versus shear strain obtained for repeated cyclic loading, in dynamic and static tests on soil tested dry (Bolton and Wilson, 1989). Torque T and rotation θ were measured directly in the static tests. Shear strain in Fig. 3 was referred to the circumference of the solid sample ($\gamma \approx \theta/4$). The resonant column tests were analysed by treating the system as having one degree of freedom, θ. The moment of inertia I of the top cap was about 100 times greater than that of the soil, so the sample only contributed stiffness and damping. At resonance, the inertial torque driving the oscillation can be taken to be $I\ddot{\theta}$. The measurement of $\ddot{\theta}$ at the observed resonant frequency therefore led directly to the establishment of a point on the backbone curve. Each point in Fig. 3 represents the amplitude of shear strain variations measured after several cycles of torque of a given amplitude. It is therefore possible to move along the backbone curve only if there are no additional plastic strains involved in the creation of the steady cyclic response.

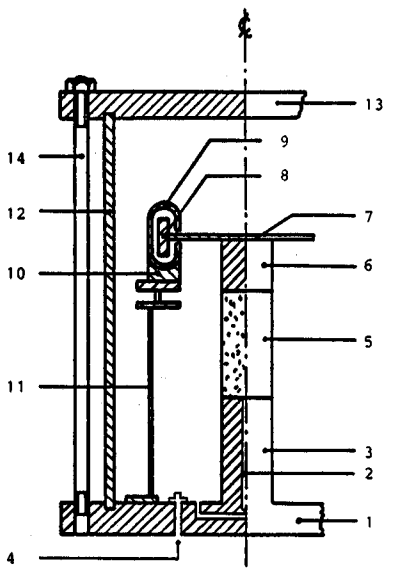

Fig.1 Stokoe resonant column apparatus

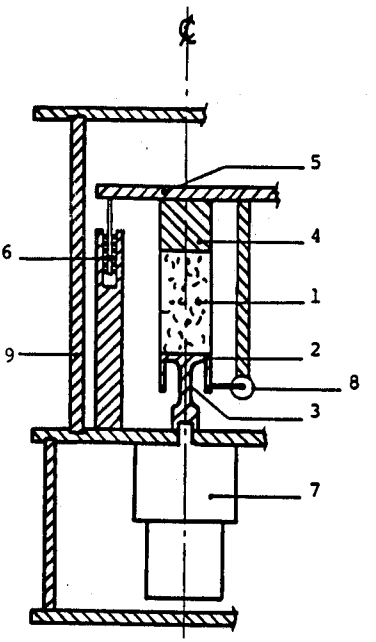

Fig.2 Wilson apparatus for slow, cyclic torsion

Fig. 4 shows that the imposition of a cyclic torque may produce a permanent plastic deformation, which in the case of dense sand is of the same order as the steady cyclic response. These permanent plastic strains are not discussed in the present paper.

Figure 3 demonstrates a good correspondence between the backbone curves of samples tested quasi-statically (0.001 Hz) and samples tested dynamically (45 to 95 Hz). It follows that dry sand must be regarded not as viscous but as hysteretic. The power dissipated in such a body is then proportional to the area of the steady hysteresis loop, muliplied by the frequency of vibration.Hardin and Drnevich (1972) show that the damping ratio D is given by $A_L / (4\pi A_T)$ where A_L is the area enclosed by the loop and A_T is the area enclosed by the triangle the base of which is the rotation amplitude and the height of which is the torque amplitude. The two methods of deriving damping ratio, via decay decrement for dynamic tests and via hysteresis loop area for static tests, are used in Fig. 5 to portray energy dissipation in dry sand. This confirms that damping in dry sand is purely hysteretic and independent of testing frequency.

4 CYCLIC DATA FOR SATURATED SAND

Dynamic torsion tests were carried out on samples poured dry as before, but subsequently saturated with pore fluid. The degree of saturation was established by performing B-tests, in which the ratio of pore pressure response to cell pressure increment was measured over a range of increments. Isolation of the sample was also checked, and it was found necessary to bathe the outside of the membrane in the appropriate cell fluid to avoid air migration into the specimen from the pressure chamber. Water saturation in two early tests was not perfect as revealed by B-values less than 0.9. Improvements were made by first flushing the sample with carbon dioxide, then applying a strong vacuum before drawing de-aired water through the sample, prior to testing under a back-pressure of 200 kPa. Oil-filled specimens were similarly saturated with silicone oil of viscosity 100 times that of water. B-values of 0.90 to 0.99 were then achieved. All the samples were drained during testing.

Fig. 6 compares the dynamic torsion data of dry (D), water- (W) and oil-saturated (O) samples at mean effective stresses of about 100 and 300 kPa. It is evident that the presence of these pore fluids had little effect on secant soil stiffness at shear strains up to 10^{-3}. Damping provides the most accurate measure of non-linearity, however, and Fig.7 shows that water failed to make any extra contribution, whereas silicone oil increased the damping ratio by a factor of 2 to 3. Figures 5,6 and 7 are based on the data of Wilson (1988) supplemented by the findings of a confirmatory study by Skinner (1990). In both studies, the damping with pore oil varied more than usually from sample to sample.

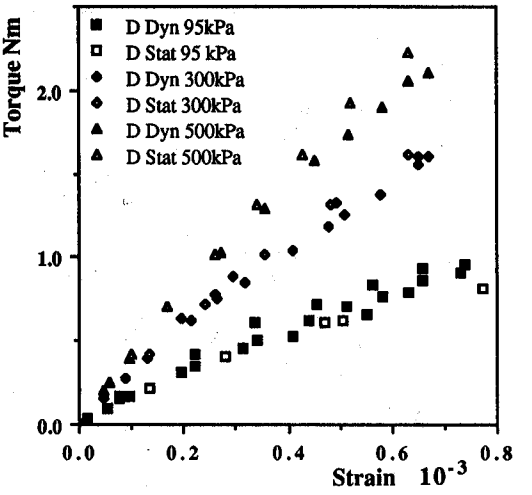

Fig.3 Static and dynamic torsion of dry sand

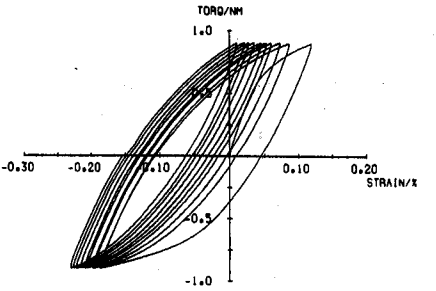

Fig.4 Hysteresis loops for dry sand in static test

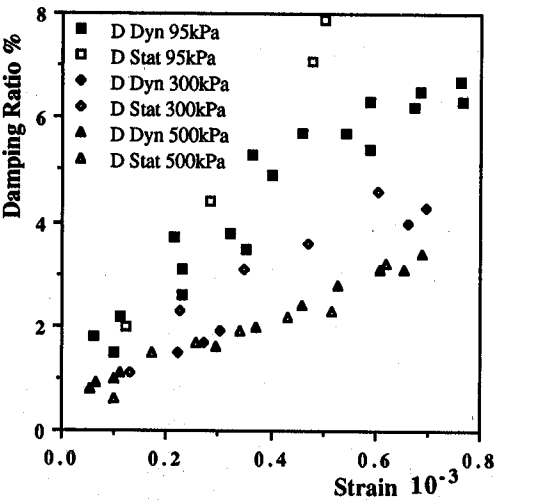

Fig.5 Static and dynamic damping, dry sand

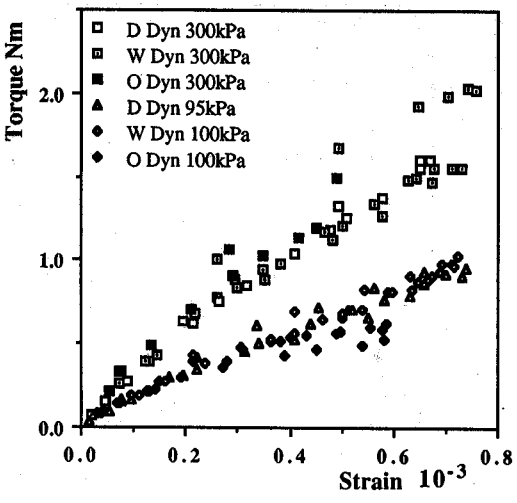

Fig.6 Backbone data, dry and fluid-saturated sand

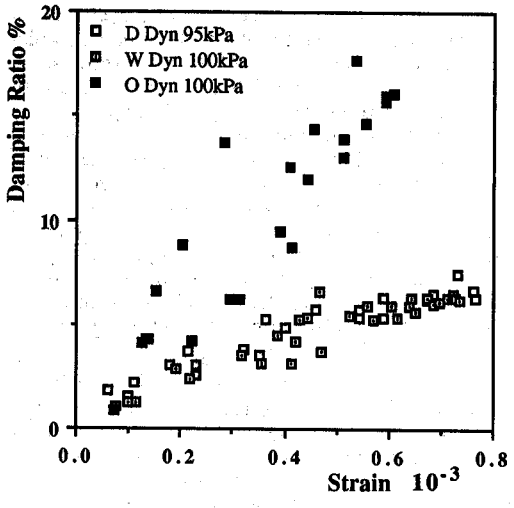

a) Tests circa p'= 100 kPa

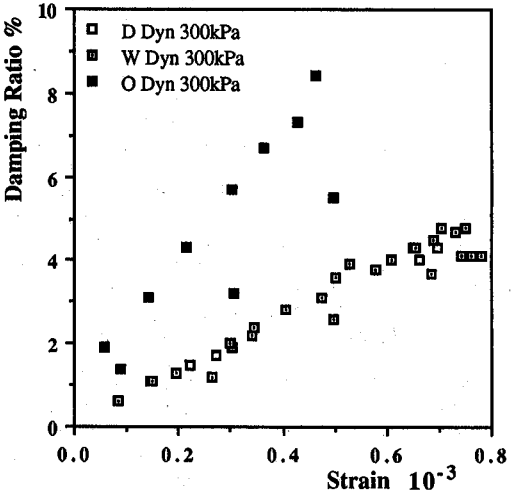

b) Tests circa p'= 300 kPa

Fig.7 Damping in dry and fluid-saturated sand

Since the situations in which soil damping will be required in practice are rather varied, it is necessary to consider the possible combined effects of fluid viscosity and applied frequency for which a pore fluid may exert some influence on damping. It may then be possible to judge whether any measured effects are likely to be the result of hydrodynamic drag, or some other cause.

5 ANALYSIS OF FLUID DAMPING IN SOILS

It is desirable to have an order-of-magnitude estimate of the possible effects of viscous damping due to the pore fluid. Consider first a unit cube of pore fluid of dynamic viscosity η, subject to a rate of shear $\dot{\gamma}$. The instantaneous drag on its top surface would be $\eta\dot{\gamma}$ and the rate of work of this drag would represent the instantaneous power loss in viscous damping within the element, which would be

$$P = \eta\ \dot{\gamma}^2 \qquad (1)$$

Now consider the possible influence of soil particles. Although there may be no net volume change, fluid will be forced to flow around the moving soil particles, as voids open and close. If the typical velocity of one particle relative to another is $\dot{\gamma}d$, the root mean square relative fluid velocity necessary to clear a void for the particle to enter may be $\lambda\dot{\gamma}d$, where λ is a dimensionless measure of the void constriction, averaged over the gross volume. For example, if a particle of diameter d moving at velocity v were constricted only by fluid in 3 "semi-circular canals" each of effective internal diameter d/5, the absolute velocity of the fluid would be v.$5^2/3$, so that the relative velocity would be about 9v. If the soil had void ratio e, the superficial relative velocity would be about 9ve/(1+e) which gives a value $\lambda \approx 3$.

Random hydraulic gradients of the order $\lambda\dot{\gamma}d/k$ (where k is Darcy's permeability) will therefore be induced by the deformation of the soil. If a unit cube were to be subject to a uniaxial hydraulic gradient i in fluid of mass density ρ, the loss of pressure across it would be $i\rho g$. The associated rate of dissipation of energy in viscous friction would be this pressure

differential multiplied by the flow rate, giving $i^2 k \rho g$. If it is assumed that the same order of dissipation would occur with random flow , this can now be written

$$P = \lambda^2 \dot{\gamma}^2 d^2 \rho g / k \qquad (2)$$

Of course, it is advisable to substitute a more fundamental group of parameters for Darcy's permeability k. This can be done through Poiseuille's idealisation of laminar flow in tubes, in conjunction with Allen Hazen's empirical correlations for sands:

$$k = \frac{10^{-3} d^2 \rho g}{\eta} \qquad (3)$$

where all quantities are in SI units (m, kg, s, N) and the order of magnitude is consistent with measurements on the dense sand under investigation. On substituting (3) into (2), we obtain

$$P = 10^3 \lambda^2 \eta \dot{\gamma}^2 \qquad (4)$$

which is perhaps four orders of magnitude larger than that for a simple fluid element, given in equation (1).

It remains to find the energy dissipation E_v per unit volume due to viscous damping over one cycle of shear strain $\gamma = \gamma_a \sin \omega t$ so that $\dot{\gamma} = \gamma_a \omega \cos \omega t$ and

$$E_v = \pi \times 10^3 \eta \lambda^2 \gamma_a^2 \omega \qquad (5)$$

Hysteretic energy dissipation E_h has already been shown to be the area of the effective stress-strain loop, and damping ratio D has been defined as $1/4\pi$ times the total dissipation per cycle divided by the energy E_t defined as the area of the triangle beneath the radius from the origin to the turning point (τ_a, γ_a) of the loop (sometimes loosely termed the strain energy stored per cycle). We can write

$$E_t = 0.5 \tau_a \gamma_a = 0.5 G \gamma_a^2 \qquad (6)$$

where G is the secant modulus at the turning point. Then if damping ratio D is partitioned into D_h due to true hysteresis and D_v due to viscosity in the pore fluid, we obtain:

$$D = D_h + D_v = (E_h + E_v)/(4\pi E_t) \qquad (7)$$

or

$$D = D_h + 0.5 \times 10^3 \lambda^2 \frac{\eta \omega}{G} \qquad (8)$$

It would seem useful to preserve the dimensionless terms of (8) and to define a dimensionless fluid dissipation factor F_v such that the fluid component of damping ratio is given by

$$D_v = F_v \frac{\eta \omega}{G} \qquad (9)$$

where F_v has been estimated to be about 0.5×10^4. If we substitute notional values $\eta = 10^{-6}$ kNs/m^2 for water, $\omega = 150\pi$ corresponding to 75 Hz, and G = 10^5 kN/m^2 for small amplitude vibrations, we get a predicted viscous damping component $D_v \approx 2 \times 10^{-5}$ which would be entirely negligible.

Fig.7 confirms that water filling the pores of sand in the resonant column tests had a negligible effect on the damping ratio. However, Fig.7 also shows that oil of only 100 times greater viscosity does have a significant effect. Three remarks may be made.

First, if the typical extra damping ratio is $D_v \approx 0.05$ with oil of viscosity $\eta = 10^{-4}$ kNs/m^2, we deduce that $\lambda \approx 15$ if (8) applies. This value is much higher than that which was inferred using the damping mechanism of flow in channels. It is possible that the greater dissipation is due to fluid being expelled from points of contact between soil particles, but the roughness of the asperities suggests otherwise.

Second, Fig.7 shows that D_v is roughly proportional to strain amplitude. The progressive reduction in G evident in Fig.6 is not sufficient to explain this phenomenon through (9). The only way of retaining the fluid viscosity explanation would be to infer that F_v increases with shear strain, due to the progressive disturbance of the soil fabric. A more persuasive explanation would involve the surface lubrication of sand particles due to adhesion of silicone molecules, leading to the destabilization of contacts under tangential forces, and the enhancement of hysteretic strains (and therefore damping) for the aggregate. It is then necessary to ascribe greater curvature to the backbone curves of sand with oil: Fig. 6. By this argument, oil viscosity effects would only enter at frequencies much higher than 100 Hz.

Third, those who model earthquake effects by centrifuging 1/n scale soil models at n gravities, replacing ground water by an oil of n times the viscosity, and replicating field accelerations but at n times their frequency, should be aware that significant differences in damping ratio have been found in oil and water-saturated elements of sand tested under identical conditions. It would be prudent to check observations on oil-saturated models using an alternative water-saturated model. It would still be necessary to reduce soil permeability by a factor n: this could be attempted by scaling soil particles down in size by $\sqrt{n}$. A cyclic test would be necessary to confirm that the alternative soils possessed similar stiffness and damping parameters.

Care should be taken not to extrapolate damping ratios beyond the range of soil and fluid states, and excitations, for which they were measured. Further

work is obviously necessary. It is, however, clear that water-saturated sand is purely hysteretic at typical earthquake frequencies.

6 FREQUENCY RESPONSE

It has been shown that water-saturated quartz sands behave purely hysteretically at frequencies upto about 100Hz, and it has been hypothesised that the same would apply beyond 1 kHz, and irrespective of particle size. Bolton and Wilson (1989) have shown that the frequency response of a hysteretic soil system is highly sensitive just below resonance, and that this effect may be predicted for a single-degree-of-freedom system using established techniques of non-linear vibration analysis. Many resonance problems, whether of machine bases subject to out-of-balance forces or of piled foundations in earthquakes, might be regarded directly as capable of representation as 1°F systems. Others, such as dams in earthquakes, might be treated as 1°F systems if their mode of vibration could be predicted with sufficient accuracy.

The 1°F analysis of a solid circular cylinder of hysteretic soil in first mode torsional vibration may therefore be taken as an example of a wider class of investigation. The equation of motion may be written:

$$I\ddot{\theta} + f(\theta, \text{sign } \dot{\theta}) = T_a \cos \omega t \qquad (10)$$

where $f(\theta, \text{sign } \dot{\theta})$ represents the torque necessary to achieve a top-cap rotation θ on a stable hysteresis loop obtained after sufficient cycles of load: Fig.4. The sign of $\dot{\theta}$ arises through the necessity to distinguish the upper (loading) and lower (unloading) paths.

This can be compared with the motion of a standard linear visco-elastic system by using a decomposition suggested by Kryloff and Bogoliuboff, and given in English by Minorsky (1947):

$$I\ddot{\theta} + c\dot{\theta} + k\theta + E(\theta, \text{sign } \dot{\theta}) = T_a \cos \omega t \qquad (11)$$

Best-fit equivalent linear parameters c and k can then be chosen to minimize the r.m.s value of the "error" E, given by

$$E = f - c\dot{\theta} - k\theta \qquad (12)$$

following Iwan and Patula (1972). Since the result will be a function of the amplitude of rotation θ_a, the method should be capable of predicting the non-linear frequency response, if an acceptable analytic form can be found for function f. Perhaps the most direct approach would be separately to fit a family of functions to each of a nest of stable hysteresis loops of different sizes. This would, however, be cumbersome.

Wilson (1988) suggested an alternative procedure for the deduction of hysteresis function f from the shape of the backbone curve joining the limit points of stable loops. Following Iwan (1966) the resistance of the soil is represented by a parallel array of Jenkin elements, each of which comprises a spring in series with a frictional slider: Fig.8. Each spring has the same stiffness K, but the yield rotations θ_y of the sliders are represented by the probability density function ρ so that torque T can be written:

$$T = K \int_0^{\theta} \theta_y \rho \, d\theta_y + K\theta \int_{\theta}^{\infty} \rho \, d\theta_y \qquad (13)$$

The first term represents the elements which have already yielded (i.e. $\theta > \theta_y$) and the second represents those that still retain their elastic stiffness K (i.e. $\theta < \theta_y$). Net stiffness is due only to the second term, so that on differentiating twice we get, first:

$$dT/d\theta = K \int_{\theta}^{\infty} \rho \, d\theta_y \qquad (14)$$

and then,

$$d^2T/d\theta^2 = -K\rho \qquad (15)$$

The probability density function of yield rotations can therefore be calculated from the curvature of the backbone curve, divided by its initial gradient.

Hardin and Drnevich (1972) showed that shear stress-strain curves approximate to hyperbolae, and a similar relation will now be assumed for the shape of a backbone curve of T versus θ,

$$T = \frac{K\theta}{(1 + \theta/\theta_r)} \qquad (16)$$

where θ_r is the reference strain, a constant for the curve, and taken to be a function of soil density and mean effective stress. Equation (16) can be rewritten:

$$\frac{K}{T} = \frac{1}{\theta} + \frac{1}{\theta_r} \qquad (17)$$

and Fig.9 shows the fit achieved on a graph of 1/T versus 1/θ with a reducing sequence of turning points defining the backbone curve of a static test on the dense sand under p' = 300 kPa, giving K = 840 Nm/rad and $\theta_r = 8.4 \times 10^{-3}$.

Having established (17) as a good analytical fit to the backbone data, double differentiation followed by substitution in (15) gives an expression for the probability density function of yield rotations:

$$\rho = \frac{2}{\theta_r (1 + \theta/\theta_r)^3} \qquad (18)$$

This then permits the derivation of function f describing a hysteresis loop with rotation amplitude θ_a. The torque following unloading from θ_a to $\theta_a > \theta > -\theta_a$ can be written in three terms, the first dealing with elements which were still elastic at θ_a and which are therefore still elastic, the second dealing with elements which had yielded but which have now become elastic again, and the third dealing with elements which had yielded on loading and which have already yielded on unloading:

$$T = K\theta \int_{\theta_a}^{\infty} \rho \, d\theta_y + K \int_{(\theta_a-\theta)/2}^{\theta_a} (\theta - \theta_a + \theta_y)\rho \, d\theta_y - K \int_{0}^{(\theta_a-\theta)/2} \theta_y \rho d\theta_y \quad (19)$$

A similar expression for the reloading leg confers symmetry, and completes the derivation of the hysteresis loop. Fig.8 simulates the process with just three Jenkin elements.

Wilson (1988) goes on to minimise the error term, equation (12), and to derive the following best-fit equivalent linear parameters for the case of a hyperbolic backbone curve:

$$k = \frac{4K}{\alpha (1+\alpha)^2} \quad (20)$$

$$c = \frac{4K}{\pi\omega}\left(\frac{\ln\alpha^4}{(\alpha^2-1)^2} - \frac{(\alpha^2+1)}{\alpha^2(\alpha^2-1)} \right) \quad (21)$$

where

$$\alpha^2 = 1 + \frac{\theta_a}{\theta_r} \quad (22)$$

Equations (20), (21) and (22) can be used to obtain the dynamic response from equation (11), treating the minimized "error" term E as zero. The standard solution $\theta = \theta_a \cos(\omega t - \phi)$ gives:

$$\theta_a = \frac{T_a}{\sqrt{(k - I\omega^2)^2 + c^2\omega^2}} \quad (23)$$

but both k and $c\omega$ are here functions of θ_a. Figure 10 shows the comparison between the dynamic response measured in resonant column tests on dry sand at a mean effective stress of 300 kPa, and that predicted from (23) based on a quasi-static backbone curve. At each frequency ω and excitation T_a, an iteration was performed to solve for θ_a from (23). Similar results were obtained for water and oil-saturated sand.

It will be appreciated that the correspondance is close enough to encourage the similar analysis of more complex soil systems. Of particular significance

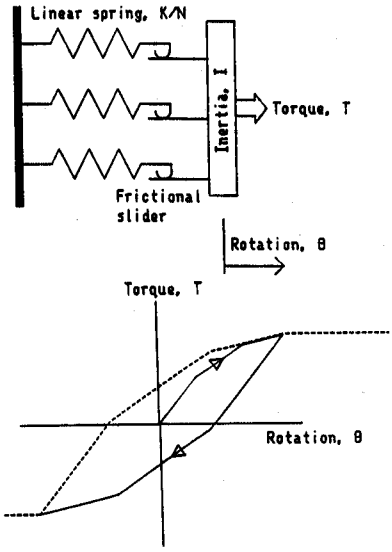

Fig.8 Iwan-Jenkin model of hysteresis

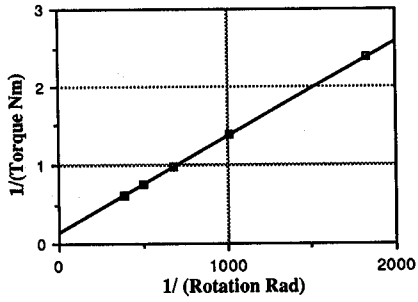

Fig.9 Hyperbolic curve-fit for test 8 backbone

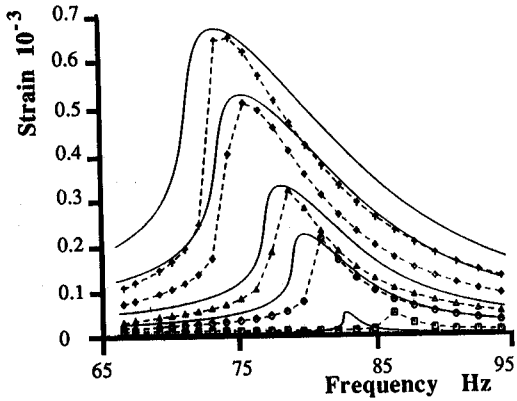

Fig.10 Predicted and measured response curves

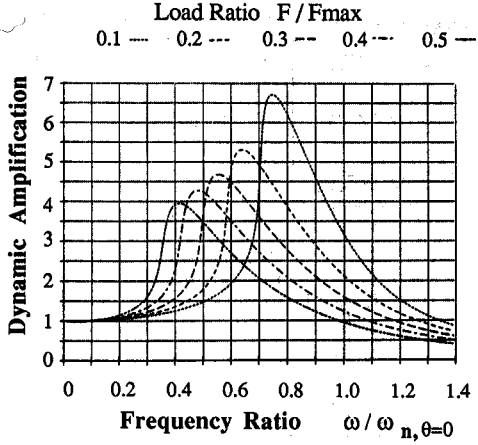

Fig. 11 Hysteretic system response predictions (hyperbolic backbone)

is the extreme sensitivity to frequency just below resonance, and the reduction of resonant frequency with response amplitude. These predictions using hyperbolae are similar to those previously reported using cubic backbone curves (Bolton and Wilson, 1989). Hyperbolae offer significant advantages for the prediction of non-linear behaviour when the small-strain stiffness K and system inertia I can be used to find the small-strain natural frequency $\omega_{n,\theta=0} = \sqrt{K / I}$, and where the peak strength F_{max} can separately be estimated. Figure 11 is a dimensionless plot of dynamic amplification ($\theta_{a,\omega} / \theta_{a,\omega=0}$) versus frequency ratio ($\omega / \omega_{n,\theta=0}$), at various load ratios (F / F_{max}).

7 CONCLUSIONS

Stiffness and damping parameters of sand are insensitive to whether they have been measured in quasi-static or dynamic tests upto 100 Hz, and whether the samples are dry or water-saturated. All such behaviour is hysteretic, and parameters are strain dependent but are independent of frequency.

A higher damping ratio has been observed in sand saturated with silicone oil of 100 cS viscosity, at about 75 Hz. The effect was approximately to treble the hysteretic damping measurable on dry sands, possibly through boundary lubrication. An approximate analysis of energy dissipation due to fluid viscosity threw up the dimensionless group $\eta\omega/G$, but was unable to match either the form or magnitude of the data. For the present, material damping in oil-saturated sands should be measured at appropriate strain amplitudes and frequencies.

The dynamic behaviour of hysteretic soil systems is different from that of viscous systems, even when best-fit stiffness and damping values have been selected. In particular, a hysteretic system shows a sensitivity to frequency just below resonance which mimics that of a viscous system with an order of magnitude less damping. Hyperbolic backbone curves of excitation amplitude versus response amplitude can be used to make simple predictions. These were reasonably accurate for a cylinder excited in torsion.

8 REFERENCES

Abbiss C.P. 1986. The effects of damping on the interpretation of geophysical measurements. Geotechnique, 36, No.4, 565-580.

Bolton M.D. & Wilson J.M.R. 1989. An experimental and theoretical comparison between static and dynamic torsional soil tests. Geotechnique, 39, No.4, 585-599.

Hardin B.O. & Drnevich V.P. 1972. Shear modulus and damping in soils: design equations and curves. J. Soil Mechs. Div. Am.Soc.Civ.Engrs., 98, SM7, 667-692.

Iwan W.D. 1966. A distributed element model for hysteresis and its steady state dynamic response. J. Appl. Mechs. Am. Soc. Mech. Engng., 88, Series E, No.4, 893-900.

Iwan W.D. & Patula E.J. 1972. The merit of different error minimization criteria in approximate analysis. J. Appl. Mechs. Am. Soc. Mech. Engng., 94, Series E, No.1, 257-262.

Iwasaki T., Tatsuoka F. & Takagi Y. 1978. Shear moduli of sands under cyclic torsional shear loading. Soils and Foundations, 18, No.1, 39-56. Tokyo.

Minorsky N. 1947. Introduction to non-linear mechanics. Michigan: Ann Arbor.

Skinner H.D. 1990. The effect of pore fluid on the dynamic properties of sand. Project report, Engineering Tripos Part II, Cambridge University, U.K.

Wilson J.M.R. 1988. An experimental and theoretical investigation into the dynamic behaviour of soils. Ph.D. dissertation, Cambridge University, U.K.